Tarantula Toxins Interact with Voltage Sensors within Lipid Membranes

Mirela Milescu,[1] Jan Vobecky,[1] Soung H. Roh,[2] Sung H. Kim,[2] Hoi J. Jung,[2] Jae Il Kim,[2] and Kenton J. Swartz[1]

[1]Molecular Physiology and Biophysics Section, Porter Neuroscience Research Center, National Institute of Neurological Disorders and Stroke, National Institutes of Health, Bethesda, MD 20892

[2]Department of Life Science, Gwangju Institute of Science and Technology, Gwangju, 500-712, Korea

Voltage-activated ion channels are essential for electrical signaling, yet the mechanism of voltage sensing remains under intense investigation. The voltage-sensor paddle is a crucial structural motif in voltage-activated potassium (K_v) channels that has been proposed to move at the protein–lipid interface in response to changes in membrane voltage. Here we explore whether tarantula toxins like hanatoxin and SGTx1 inhibit K_v channels by interacting with paddle motifs within the membrane. We find that these toxins can partition into membranes under physiologically relevant conditions, but that the toxin–membrane interaction is not sufficient to inhibit K_v channels. From mutagenesis studies we identify regions of the toxin involved in binding to the paddle motif, and those important for interacting with membranes. Modification of membranes with sphingomyelinase D dramatically alters the stability of the toxin–channel complex, suggesting that tarantula toxins interact with paddle motifs within the membrane and that they are sensitive detectors of lipid–channel interactions.

The Journal of General Physiology

INTRODUCTION

Voltage-dependent cation channels open and close in response to changes in the membrane voltage, a property that is essential for the generation and propagation of rapid and long-range electrical signaling within the nervous system. These channels have a modular architecture, with a central pore domain that determines ion selectivity, and four surrounding voltage-sensing domains that move in response to changes in membrane voltage and drive opening of the pore (Kubo et al., 1993; Doyle et al., 1998; Li-Smerin and Swartz, 1998; Lu et al., 2001; Jiang et al., 2003a). Although X-ray structures have now been solved for two voltage-activated potassium (K_v) channels (Jiang et al., 2003a; Lee et al., 2005; Long et al., 2005), the structural basis of voltage sensing remains the subject of intense investigation. One remarkable aspect of the X-ray structures of the K_vAP channel and its isolated S1–S4 voltage-sensing domain is the presence of the voltage-sensor paddle motif, a helix-turn-helix structure that is comprised of the S3b helix and the charge-bearing S4 helix (Jiang et al., 2003a; Lee et al., 2005; Long et al., 2005). In the K_vAP structures, as well as the more recent K_v1.2 structure, the voltage-sensor paddle is predicted to be buried in the membrane and positioned at the protein–lipid interface (Jiang et al., 2003a,b; Ruta et al., 2003; Cuello et al., 2004; Lee et al., 2005; Ruta et al., 2005; Schmidt et al., 2006), which is conceptually distinct from the conventional models where the S4 charges are protected from membrane lipids by other parts of the protein (Ahern and Horn, 2004; Tombola et al., 2005).

A particularly intriguing aspect of the voltage-sensor paddle motif is that venomous creatures synthesize protein toxins that interact with this motif and thereby modify voltage-dependent gating. For example, hanatoxin is a tarantula toxin that inhibits the K_v2.1 channel by interacting with the S3b and S4 helices, and stabilizing the voltage sensors in a resting conformation (Swartz and MacKinnon, 1997a,b; Li-Smerin and Swartz, 2000, 2001; Lee et al., 2003; Phillips et al., 2005; Swartz, 2007). Related toxins from spiders, scorpions, and sea anemone also target the equivalent regions of voltage-activated sodium (Na_v) and calcium (Ca_v) channels (Rogers et al., 1996; Cestele et al., 1998; Li-Smerin and Swartz, 1998; Winterfield and Swartz, 2000; Cestele et al., 2006). Such widespread targeting of the paddle motif by venom toxins is consistent with the idea that the paddle is a uniquely mobile part of the voltage-sensing domain, as suggested by functional studies on the K_vAP channel (Ruta et al., 2005). The proposed location of the paddle motif at the protein–lipid interface raises the possibility that the target of voltage-sensor toxins is buried in the membrane, and that these toxins interact with the channel within the lipid bilayer.

Several tarantula toxins have been shown to partition into model membranes containing anionic lipids, including VSTx, GsMTx-4, ProTx-II, and hanatoxin

Correspondence to Mirela Milescu: milescum@ninds.nih.gov; or Kenton J. Swartz: swartzk@ninds.nih.gov

Abbreviations used in this paper: CD, circular dichroism; LUV, large unilamellar vesicle; PB, physiological buffer; POPC, 1-palmitoyl-2-oleoyl-sn-glycero-3-phosphocholine; POPG, 1-palmitoyl-2-oleoyl-sn-glycero-3-[phospho-rac-(1-glycerol)]; SM, sphingomyelin; SMaseD, sphingomyelinase D; WT, wild type.

(Lee and MacKinnon, 2004; Suchyna et al., 2004; Jung et al., 2005; Phillips et al., 2005; Smith et al., 2005). The structures of these toxins are highly amphipathic (see Fig. 1, A and B), with one face containing a cluster of hydrophobic residues surrounded by polar residues, most of which are basic (Takahashi et al., 2000; Lee et al., 2004). These structural features, together with previous depth-dependent fluorescence quenching experiments (Phillips et al., 2005) and molecular dynamics simulations (Bemporad et al., 2006; Wee et al., 2007), point to a relatively superficial position of these toxins in model membranes and raise the possibility that partitioning may be very sensitive to the presence of charged moieties on phospholipid membranes. Anionic lipids are scarce in the external leaflet of native membranes (Simons and van Meer, 1988; Calderon and DeVries, 1997; Hill et al., 2005), the side from which these toxins act, and thus it is crucial to understand whether tarantula toxins can partition into native membranes containing an abundance of zwitterionic lipids. Indeed, recent studies have questioned whether membrane partitioning is involved in the inhibitory mechanisms for toxins that modify gating of voltage-activated ion channels (Cohen et al., 2006; Posokhov et al., 2007b). In the case of GsMTx-4, partitioning of the toxin has been proposed to alter lipid packing around stretch-activated cation channels, and thus to inhibit channel activity without the toxin specifically binding to the channel protein (Suchyna et al., 2004). In a related fashion, might partitioning of tarantula toxins be sufficient for altering the activity of K_v channels? If tarantula toxins do interact directly with the channel, which regions of the toxin are involved in protein–protein interactions and which are important for their interactions with membranes? Finally, are interactions of these toxins with membranes required for inhibition of K_v channels? We set out to address these fundamental questions for hanatoxin and SGTx1, two closely related tarantula toxins that inhibit the $K_v2.1$ channel. We characterized partitioning of these toxins into membranes of varying composition using fluorescence and separation methods, and synthesized the D-enantiomer of SGTx1 to address whether toxin-induced perturbations of the bilayer are sufficient to inhibit the channel. To define regions of tarantula toxins that are important for interacting with membranes and voltage-sensor paddles, we studied the effects of SGTx1 mutations on membrane partitioning and on the concentration dependence of toxin occupancy of the channel. We also examined the effects of membrane modifications on the stability of the toxin–channel complex. Our results suggest that tarantula toxins interact with the paddle motif within the lipid membrane and that modification of the lipid membrane can have dramatic effects on the toxin–channel interaction.

MATERIALS AND METHODS

Toxin Production

Hanatoxin was purified from *Grammostola spatula* venom (Spider Pharm) as previously described (Swartz and MacKinnon, 1995). WT and mutants of SGTx1 were synthesized using an Applied Biosystems model 433A peptide synthesizer. The linear precursors were synthesized using solid-phase methodology with Fmoc chemistry, starting from Fmoc-Phe-Alko resin using a variety of blocking groups for the protection of the amino acids. After trifluoroacetic acid cleavage, a crude linear peptide was extracted with 2 M acetic acid and diluted to a final concentration of 25 μM. A solution containing 0.1 M ammonium acetate, 2 M urea, and 2.5 mM reduced/0.25 mM oxidized glutathione was adjusted to pH 7.8 with aqueous NH_4OH and stirred slowly at 4°C for 3 d. The folding reaction was monitored with RP-HPLC, and the crude oxidized product was purified by successive chromatography steps with CM-cellulose CM-52 and preparative RP-HPLC with a C18 silica column. The purity of the synthetic SGTx1 was confirmed by analytical RP-HPLC and MALDI-TOF-MS measurements. The concentration of SGTx1 was determined from dry weight of the protein. To confirm toxin concentration we also measured absorbance at 280 nm and calculated the concentration of the toxin using an extinction coefficient of $8.6 \times 10^3\ M^{-1}cm^{-1}$ (Gill and von Hippel, 1989). With the exception of W30A, a mutation that removes the only Trp, concentrations determined from dry weight were within 5% of those determined from absorbance. Circular dichroism (CD) spectra were examined for each mutant to establish that the correct fold had been obtained and examples for each have been published previously (Wang et al., 2004). D-SGTx1 was synthesized using D-enantiomer Fmoc precursors.

Circular Dichroism Measurements of SGTx1

The CD spectra of D- and L-SGTx1 were obtained using a JASCO J-715 spectrophotometer (20 mM sodium phosphate buffer, pH 7.0) at 25°C with a quartz cell of 1 mm path length. Wavelengths from 190 to 250 nm were measured at 50 nm/min; the step resolution was 0.1 nm, the response time 0.5 s, and the bandwidth 1 nm. Spectra were collected and averaged over four scans. The mean residue ellipticity [θ] ($deg{\cdot}cm^2{\cdot}dmol^{-1}$) was calculated as $[\theta] = [\theta]_{obs}(MRW/10lc)$, where $[\theta]_{obs}$ is the ellipticity measured in millidegrees, MRW is the mean residue molecular weight of the peptide, c is the concentration of the sample in mg/ml, and l is the optical path length of the cell in cm. The spectra are expressed as molar ellipticity [θ] vs. wavelength.

Preparation of Lipid Vesicles

Phospholipids were dried from a chloroform solution under a nitrogen stream. The dried lipid film was rehydrated in buffers used for the partitioning assay: HEB (10 mM HEPES, 1 mM EDTA, pH 7.0 with NaOH) with or without 100 mM KCl and 2 mM $CaCl_2$ (1 mM free Ca^{2+}; Patton et al., 2004); and physiological buffer (PB) (10 mM HEPES, 100 mM KCl, 1 mM $MgCl_2$, 0.3 mM $CaCl_2$, pH 7.6 with NaOH). The resulting dispersions were extruded through 100 nm pore size polycarbonate filters (Millipore Corp.) to form large unilamellar vesicles (LUVs).

Fluorescence Spectroscopy

All fluorescence measurements were performed in quartz cuvettes with 1 cm path length. LUVs composed of POPC (1-palmitoyl-2-oleoyl-sn-glycero-3-phosphocholine) or a mix of 1:1 molar ratios of POPG (1-palmitoyl-2-oleoyl-sn-glycero-3-[phospho-rac-(1-glycerol)]) and POPC were added to a solution of toxin (2 μM final concentration of toxin), maintained at 25°C with continuous stirring in a total volume of 2 ml. Fluorescence spectra (averaging three spectra) were recorded between 300 and 400 nm

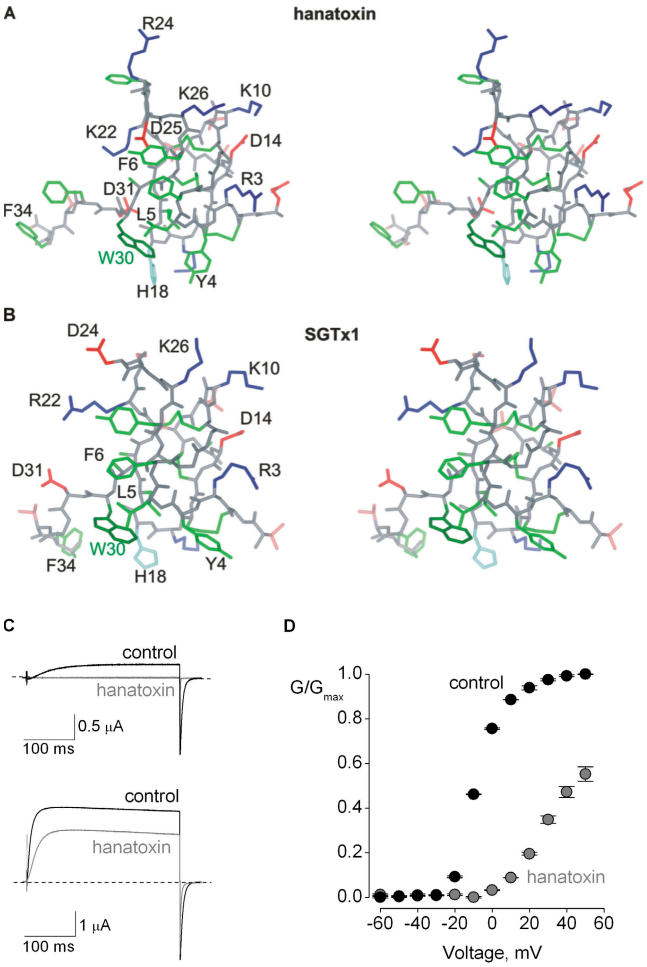

Figure 1. NMR structures of hanatoxin and SGTx1 and inhibition of the Kv2.1 channel by hanatoxin. Stereo views of hanatoxin (A) and SGTx1 (B) NMR solution structures. Side chain colors are as follows: green, hydrophobic; blue, basic; red, acidic; pink, Ser/Thr; gray, other side chains and backbone atoms. Protein database accession codes are 1D1H for hanatoxin and 1LA4 for SGTx1. (C) Voltage-clamp recording from an oocyte expressing the $K_v2.1$ channel. Currents were elicited by depolarization to −10 mV (above) or +50 mV (below), in the absence (black) or presence of 4 μM hanatoxin (gray). The holding voltage was −100 mV, and the tail voltage was −80 mV. The dashed line indicates the level of zero current. Leak, background, and capacitive currents were subtracted after blocking the channel with agitoxin-2. (D) Voltage–activation relations in the absence (black) and presence of 4 μM hanatoxin (gray). Tail currents obtained following depolarizations were averaged for 0.2 ms beginning 2 ms after repolarization to −80 mV. Data points are the mean ± SEM ($n = 3$).

(5 nm band pass, 0° polarizer) using an excitation wavelength of 280 nm (5 nm band pass, 90° polarizer) (SPEX FluoroMax 3 spectrofluorometer) and corrected for vesicle scattering (Ladokhin et al., 2000). For calculating mole-fraction partitioning coefficients (K_x), fluorescence intensity (F) at 320 nm was measured and normalized to the zero lipid fluorescence intensity (F_0). K_x was calculated based on the best fits of the following equation to the data: $F/F_0(L) = 1 + (F/F_0^{max} - 1)K_x[L]/([W] + K_x[L])$, where $F/F_0(L)$ is the change in fluorescence intensity for a given concentration of lipid, F/F_0^{max} is the maximum fluorescence increase at high lipid concentrations, [L] is the average available lipid concentration (60% of total lipid concentration), and [W] is the molar concentration of water (55.3 M). Two mutants (H18A and D31A) exhibit only very small blue shifts in λ_{max} upon addition of lipid vesicles, precluding the use of F/F_0 measurements at 320 nm to determine the fraction partitioned. In these instances, K_x values were calculated by fitting the following equation to the data: $f_p = K_x[L]/(K_x[L] + [W])$, where the fraction of toxin partitioned into the membrane (f_p) is equal to $([Toxin_{total}] - [Toxin_{free}])/[Toxin_{total}]$. $Toxin_{free}$ and $Toxin_{bound}$ were determined from the deconvolution of the emission spectra into membrane-bound and free components: $I(L) = (Toxin_{free})I_w + (Toxin_{bound})I_m$, where $I_{w(m)} = I_0\exp[(\ln 2/\ln^2\rho)\ln^2(1 + (\lambda - \lambda_{max})(\rho^2 - 1)/\rho\Gamma)]$. I(L) is the change in fluorescence intensity for a given concentration of lipid; I_w and I_m are the specific intensities for the toxin in water and in membrane, respectively; I_0 is the intensity at λ_{max}; Γ is the width at $I_0/2$; and ρ is the asymmetry of the distribution (Polozov et al., 1998; Ladokhin et al., 2000).

Quenching of tryptophan fluorescence was examined for a mixture of toxin:lipid (1:450 molar ratio; 2 μM:0.9 mM) by titration of 0.4 M acrylamide. The Stern-Volmer quenching constant (K_{SV}) was calculated based on the best fits of the following equation to the data: $F_0/F = 1 + K_{SV}[Q]$, where F_0 and F are fluorescence of the toxin in the absence and presence of acrylamide, and [Q] is the concentration of acrylamide.

Toxin Depletion Assays

Varying amounts of lipid vesicles or 300 defolliculated *Xenopus laevis* oocytes were added to an aqueous toxin solution (10 μM) and incubated with gentle agitation for 30 min at room temperature (~22°C). For experiments with oocytes the final volume was 400 μl. LUVs were separated by centrifugation (20 min, 100,000 *g*) and the oocytes by decantation, and toxin remaining in the aqueous phase was determined using RP-HPLC with an ODS (C-18) column (4.6 × 250 mm; 5 μM, 90 Å, Beckman). Hanatoxin and SGTx1 toxins were eluted with a linear gradient of 20–80% mobile phase B over 50 min at 1 ml/min (A was 0.1% TFA in water and B was 0.08% TFA in acetonitrile). Agitoxin-2 was eluted with a linear gradient of 0–50% mobile phase B over 30 min at 1 ml/min. K_x values were calculated as $K_x = (f_p/(1 - f_p))[W]/[L]$, where $f_p = ([Toxin_{total}] - [Toxin_{free}])/[Toxin_{total}]$. We estimated that an the outer leaflet of an oocyte contains 0.15 nmol of lipid using an oocyte capacitance of 0.5 μF, a specific capacitance as 1 $\mu F/cm^2$, and a surface area per lipid of 50 $Å^2$ (Nagle and Tristram-Nagle, 2000); similar values are obtained when considering the results of phospholipid analyses (Stith et al., 2000; Hill et al., 2005).

Electrophysiological Recordings

Oocytes from *Xenopus laevis* were removed surgically and incubated with agitation for 1 h in a solution containing (in mM) 82.5 NaCl, 2.5 KCl, 1 $MgCl_2$, 5 HEPES, pH 7.6 with NaOH, and collagenase (2 mg/ml; Worthington Biochemical). Defolliculated oocytes were injected with cRNA encoding the $K_v2.1\Delta7$ K^+ channel (Li-Smerin and Swartz, 1998) and incubated at 17°C in a solution containing (in mM) 96 NaCl, 2 KCl, 1 $MgCl_2$, 1.8 $CaCl_2$, 5 HEPES, pH 7.6 with NaOH, and gentamicin (50 μg/ml, GIBCO-BRL), for 24–48 h before electrophysiological recording. Oocyte membrane voltage was controlled using an OC-725C oocyte clamp (Warner Instruments). Data were filtered at 2 kHz (8-pole Bessel) and digitized at 10 kHz. Microelectrode resistances were 0.1–0.5 MΩ when filled with 3 M KCl. For the experiments in Figs. 1 and 9 the external recording solution contained (in mM) 20 KCl, 80 NaCl, 1 $MgCl_2$, 0.3 $CaCl_2$, 10 HEPES, pH 7.6 with NaOH. For the experiments in Fig. 7, the external recording solution contained (in mM) 50 RbCl, 50 NaCl, 1 $MgCl_2$, 0.3 $CaCl_2$, 10 HEPES, pH 7.6 with NaOH. For experiments with sphingomyelinase D (SMaseD), recombinant enzyme (8 ng/μl) was added to the external recording

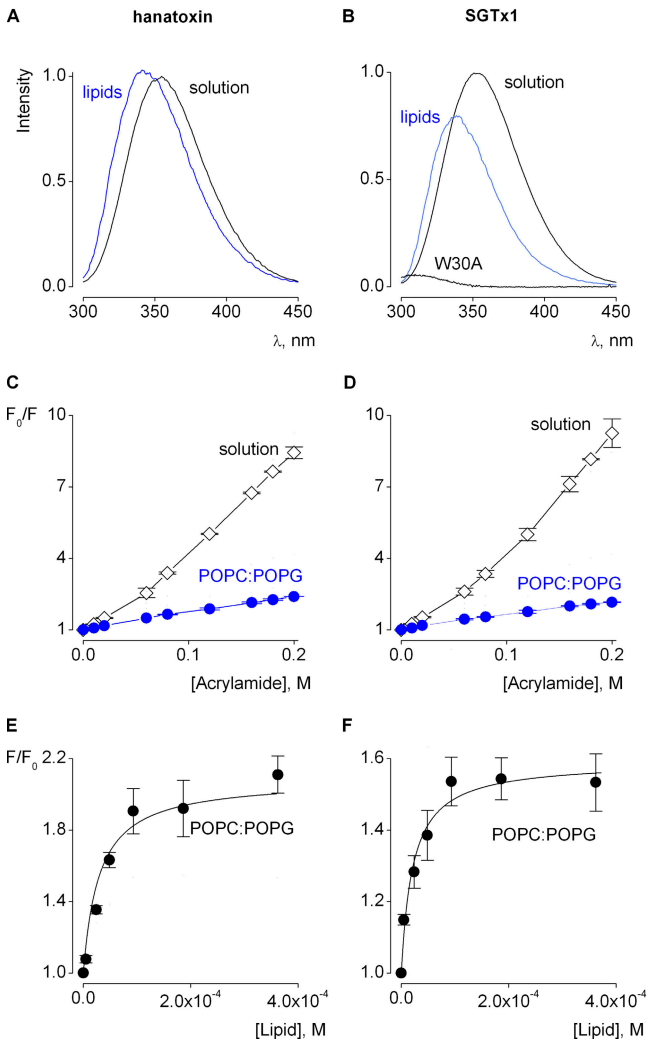

Figure 2. Interaction of hanatoxin and SGTx1 with lipid vesicles. Fluorescence emission spectra of hanatoxin (A) and SGTx1 (B) in the absence (black) or presence of lipid vesicles composed of a 1:1 mix of POPC:POPG (blue). The lipid concentration was 2.4 mM. Spectrum of W30A mutant of SGTx1 in solution is shown for comparison. Stern-Volmer plots for acrylamide quenching of W30 fluorescence of hanatoxin (C) and SGTx1 (D) in solution (2 μM, black diamonds) and in the presence of lipid vesicles (0.9 mM, blue circles). Fluorescence intensity at 320 nm plotted as a function of available lipid concentration (60% of total lipids) for hanatoxin (E) or SGTx1 (F). Smooth curves correspond to partition functions with $K_x = (4.8 \pm 0.4) \times 10^6$ and $F/F_0^{max} = 2.0 \pm 0.05$ for hanatoxin and $K_x = (3.4 \pm 0.6) \times 10^6$ and $F/F_0^{max} = 1.6 \pm 0.05$ for SGTx1. All data were obtained using HEB solution (10 mM HEPES, 1 mM EDTA, pH 7). In all cases data points are the mean ± SEM ($n = 3$).

chamber for 15–20 min and the effects on the $K_v2.1$ followed by measuring the tail current amplitudes at −80 mV elicited after depolarizations to −40 mV. After the effects on $K_v2.1$ stabilized, the enzyme was removed from the recording chamber and the cell washed extensively for 10–20 min before applying hanatoxin. All experiments were performed at room temperature (~22°C). Leak and background conductance were identified by blocking the channel with agitoxin-2 and subsequently subtracted (Garcia et al., 1994).

RESULTS

The objective of the present study is to explore whether tarantula toxins interact with lipid membranes to modify the activity of K_v channels. Previous results with VSTx1, ProTx-II, and hanatoxin, three tarantula toxins that modify the gating of K_v or Na_v channels, show that these toxins can partition quite favorably into model membranes containing anionic lipids (Lee and MacKinnon, 2004; Jung et al., 2005; Phillips et al., 2005; Smith et al., 2005). We focused our study on hanatoxin and the closely related SGTx1, two tarantula toxins of known structure (Fig. 1, A and B) that inhibit the $K_v2.1$ channel (Swartz and MacKinnon, 1997b; Takahashi et al., 2000; Lee et al., 2004; Swartz, 2007). Hanatoxin is one of the more extensively studied tarantula toxins that interacts with voltage sensors (Swartz and MacKinnon, 1997a,b; Li-Smerin and Swartz, 1998, 2000; Takahashi et al., 2000; Li-Smerin and Swartz, 2001; Lee et al., 2003, 2004; Phillips et al., 2005; Swartz, 2007), while SGTx1, unlike hanatoxin, can be efficiently folded in vitro (Lee et al., 2004), making possible the study of toxin mutants (Wang et al., 2004). Application of either toxin to the external solution bathing a cell expressing the $K_v2.1$ channel results in pronounced inhibition of opening at negative voltages, as shown in Fig. 1 (C and D) for hanatoxin, with robust opening of toxin-bound channels in response to strong membrane depolarizations.

Characterization of Toxin Partitioning into Membranes

We began by characterizing the partitioning of hanatoxin and SGTx1 into LUVs composed of a 1:1 mixture of zwitterionic (POPC) and anionic (POPG) phospholipids using intrinsic tryptophan fluorescence to monitor the toxin–membrane interaction. Both toxins contain a single solvent-accessible tryptophan residue (W30) located on the protruding hydrophobic surface (Fig. 1, A and B). When these toxins are dissolved in a simple HEB solution (10 mM HEPES, 1 mM EDTA, pH 7) and excited at 280 nm, their fluorescence emissions spectra have maxima (λ_{max}) near 353 nm (Fig. 2, A and B; Table I; Fig. 6 A), typical for tryptophan in an aqueous environment (Burstein et al., 2001; Reshetnyak and Burstein, 2001). Comparison of the emission spectra for WT and the W30A mutant of SGTx1 shows that most of the fluorescence emission originates from this single tryptophan residue (Fig. 2 B). Upon addition of lipid vesicles (2.4 mM) both hanatoxin and SGTx1 display blue shifts in their fluorescence emission spectra (Fig. 2, A and B, blue traces; Table I). A blue shift in tryptophan fluorescence is frequently observed for proteins that partition into membranes, and can be explained by a change in the polarity and rigidity of the environment surrounding the tryptophan residue (Ladokhin et al., 2000). The blue shift observed for SGTx1 (15.4 nm) is larger than for hanatoxin (10.9 nm), and the maximum fluorescence intensity decreases for SGTx1, whereas it

TABLE I

Hanatoxin and SGTx1 Partitioning into Anionic Membranes Measured Using Intrinsic Tryptophan Fluorescence

	HEB			HEB, 100 mM K^+			HEB, 100 mM K^+, 1 mM free Ca^{2+}		
Toxin	λ_{max} (nm)	K_x (10^6)	F/F_0^{max}	λ_{max} (nm)	K_x (10^5)	F/F_0^{max}	λ_{max} (nm)	K_x (10^4)	F/F_0^{max}
Hanatoxin	353.7	–	–	353.7	–	–	353.7	–	–
+POPG:POPC	342.8	4.8 ± 0.4	2.0 ± 0.05	344.3	5.3 ± 0.03	2.0 ± 0.02	350.0	4.8 ± 0.01	2.1 ± 0.1
SGTx1	352.5	–	–	352.5	–	–	352.5	–	–
+POPG:POPC	337.1	3.4 ± 0.6	1.6 ± 0.05	344.2	1.1 ± 0.01	1.7 ± 0.03	351.1	1.9 ± 0.01	2.0 ± 0.5

HEB: 10 mM HEPES, 1 mM EDTA, pH 7.

exhibits a modest increase for hanatoxin, suggesting that the tryptophan residues of the two membrane-bound toxins have distinguishable microenvironments. Similar results were obtained for the two tryptophan residues within the hydrophobic face of the related toxin GsMTx4 (Posokhov et al., 2007a). Partitioning of hanatoxin and SGTx1 into membranes can also be examined by measuring the extent to which lipid vesicles protect W30 from quenching by acrylamide, a small polar molecule that efficiently quenches tryptophan fluorescence in solution. The robust quenching of hanatoxin and SGTx1 fluorescence observed in control solutions is dramatically reduced after the addition of vesicles (Fig. 2, C and D; Table II), suggesting that in both toxins W30 is protected from the aqueous phase when these toxins interact with membranes. To characterize the strength of toxin–membrane interactions we determined mole fraction partition coefficients (K_x) from titration experiments in which the fraction partitioned was estimated by measuring changes in tryptophan fluorescence at 320 nm (F/F_0) as a function of vesicle concentration (Fig. 2, E and F) (Ladokhin et al., 2000). The maximal value of F/F_0 in the limit of high lipid concentrations (F/F_0^{max}) varies between the two toxins because the blue shift in λ_{max} and the change in maximal fluorescence intensity are different. However, fitting a partition function to the titration data reveals that the K_x values for the interaction of the two toxins with membranes composed of a 1:1 mix of POPC and POPG are similar, $(4.8 \pm 0.4) \times 10^6$ for hanatoxin and $(3.4 \pm 0.6) \times 10^6$ for SGTx1 (Table I), values indicative of relatively strong toxin–membrane interactions (Beschiaschvili and Seelig, 1990).

Next we prepared vesicles containing only the zwitterionic lipid POPC and compared the results with those obtained for vesicles containing both POPC and the anionic POPG. When high concentrations (2.4 mM) of POPC vesicles are added to aqueous solutions of hanatoxin or SGTx1 we observe much smaller blue shifts and F/F_0^{max} values compared with POPG-containing vesicles, preventing a rigorous evaluation of K_x values (Fig. 3, A–D). However, acrylamide quenching experiments show that POPC vesicles can partially protect toxin fluorescence from quenching by acrylamide (Fig. 3, E and F; Table II), suggesting that both toxins can partition into zwitterionic membranes. To estimate the strength of partitioning into zwitterionic membranes we used a toxin depletion assay in which the ability of vesicles to deplete the toxin from the aqueous phase is examined. After incubation of aqueous solutions of toxin with POPC vesicles (9 mM), the membrane-bound peptide was separated by centrifugation, and the toxin remaining in the aqueous phase quantified using HPLC. Vesicles containing POPC can deplete SGTx1 from the aqueous phase (Fig. 3 H; $f_p = 0.41 \pm 0.05$; $n = 3$), yielding a K_x value of $6.1 \pm 0.2 \times 10^3$, considerably weaker than observed for anionic membranes (Fig. 2 F; Fig. 3 G).

The importance of electrostatic interactions, revealed by a comparison of toxin partitioning into anionic and zwitterionic membranes, raises the possibility that the strength of partitioning into the external leaflet of native membranes might be rather weak. The results thus far were obtained with low ionic strength aqueous solutions without divalent ions, which would be expected to enhance the strength of partitioning compared with physiological solutions. To explore the influence of solution composition we initially examined partitioning of both toxins into anionic membranes from solutions of different composition. The K_x values for partitioning of

TABLE II

Stern-Volmer Constants for Acrylamide Quenching of Hanatoxin and SGTx1

	Stern-Volmer constant (K_{SV}), M^{-1}				
Toxin/Lipids	Solution	POPC:POPG		POPC	
		HEB	PB	HEB	PB
Hanatoxin	48 ± 3	7 ± 0.1	18 ± 0.2	10 ± 0.5	23 ± 0.7
SGTx1	38 ± 1	6 ± 0.1	26 ± 0.4	17 ± 0.3	23 ± 0.5

HEB: 10 mM HEPES, 1 mM EDTA, pH 7. PB: 10 mM HEPES, 100 mM KCl, 1 mM $MgCl_2$, 0.3 mM $CaCl_2$, pH 7.6.

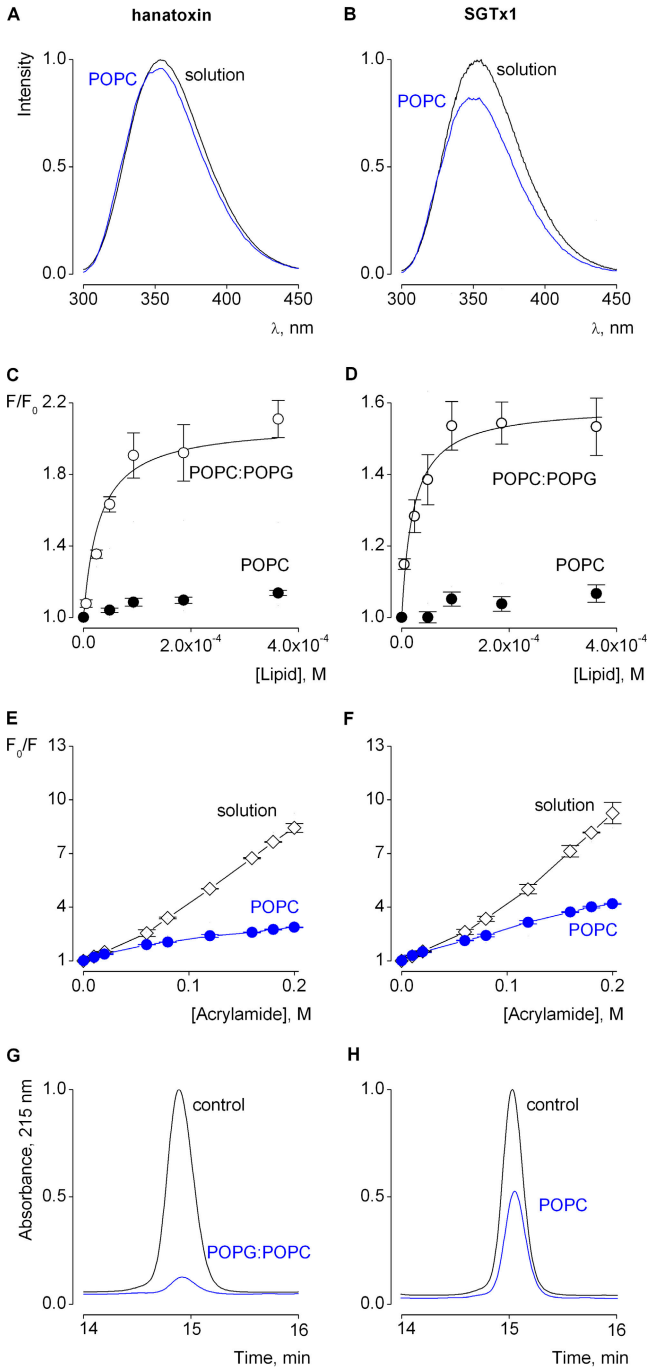

Figure 3. Effect of lipid composition on partitioning of hanatoxin and SGTx1 into lipid membranes. Fluorescence emission spectra of hanatoxin (A) and SGTx1 (B) in the absence (black) or presence of lipid vesicles composed POPC (blue). The lipid concentration was 2.4 mM. Fluorescence intensity at 320 nm plotted as a function of available lipid concentration (solid symbols) for hanatoxin (C) and SGTx1 (D). Data for vesicles containing a 1:1 mix of POPC:POPG (open symbols and smooth curves, same as in Fig. 2, E and F) is shown for comparison. Stern-Volmer plots for acrylamide quenching of W30 fluorescence of hanatoxin (E) and SGTx1 (F) in solution (2 μM, black diamonds) and in the presence of POPC vesicles (0.9 mM, blue circles). Data points are the mean ± SEM ($n = 3$). (G and H) Reversed-phase HPLC profiles of SGTx1 present in the supernatant after ultracentrifugation in the absence (black) or after addition of 9 mM lipid vesicles (blue). Traces were normalized to the maximum in the absence of lipid vesicles. All data were obtained using HEB solution (10 mM HEPES, 1 mM EDTA, pH 7).

both toxins into anionic vesicles are approximately an order of magnitude lower in an HEB solution containing monovalent cations (100 mM K^+, pH 7) compared with HEB solution alone (Fig. 4, A and B; Table I), and the addition of 1 mM free Ca^{2+} (HEB, 100 mM K^+, 2 mM $CaCl_2$, pH 7) weakens toxin partitioning even further ($K_x \sim 10^4$; Fig. 4, A and B; Table I). In a solution mimicking the electrophysiological conditions used to study the interaction of tarantula toxins with K_v channels (PB: 100 mM K^+, 1 mM Mg^{2+}, 0.3 mM Ca^{2+}, pH 7.6), the observed blue shifts and F/F_0^{max} values are too small to obtain reliable estimates of K_x (Fig. 4, A and B). To assess whether partitioning occurs under physiological ionic conditions we performed acrylamide quenching experiments, which show that W30 is partially protected from quenching by acrylamide in the presence of anionic membranes (Fig. 4, C and D; Table II). We used a similar approach to determine whether hanatoxin and SGTx1 can partition into zwitterionic membranes in the presence of physiological ionic solutions, and find that acrylamide quenching of W30 in both toxins is diminished by zwitterionic membranes (Fig. 4, E and F; Table II). Taken together, these results establish that tarantula toxins can interact with membranes under physiologically relevant conditions (e.g., zwitterionic membranes and physiological solutions).

Although the outer leaflet of native membranes contain an abundance of zwitterionic lipids, its overall composition is rather complex, including cholesterol and glycolipids, for example (Simons and van Meer, 1988; Calderon and DeVries, 1997; Hill et al., 2005). To confirm that tarantula toxins can partition into native membranes we examined the ability of intact oocytes to deplete tarantula toxins from physiological aqueous solutions (PB). When oocytes are agitated gently in a solution containing either hanatoxin or SGTx1, we consistently observe depletion of the toxins from the aqueous phase (Fig. 4 G), but not in the case of agitoxin-2, a scorpion toxin that interacts with the external vestibule of the channel (Garcia et al., 1994; Miller, 1995). The estimated K_x values for hanatoxin and SGTx1 are $\sim 10^3$ (see Materials and methods), consistent with our measurements of toxin partitioning into zwitterionic model membranes.

Structure–Function Relationships for Toxin–Membrane Interactions

To better understand the molecular basis of the interaction of tarantula toxins with membranes we examined how mutations throughout SGTx1 influence toxin partitioning into membranes. We initially used intrinsic

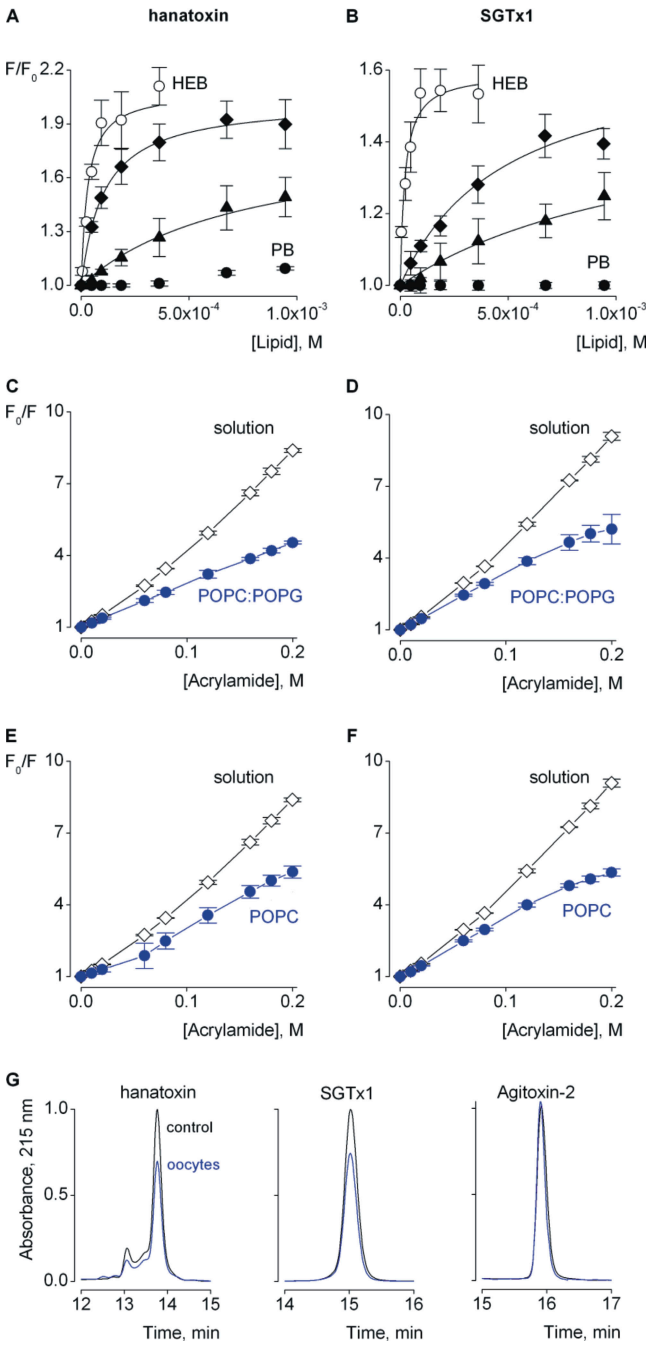

Figure 4. Effects of solution composition on partitioning of hanatoxin and SGTx1 into lipid membranes. Fluorescence intensity at 320 nm plotted as a function of available anionic lipid concentration for hanatoxin (A) and SGTx1 (B). Smooth curves are the fits of a partition function to the data as follows: diamonds for 100 mM KCl data: $K_x = (5.3 \pm 0.03) \times 10^5$ and $F/F_0^{max} = 2.0 \pm 0.02$ for hanatoxin, and $K_x = (1.1 \pm 0.001) \times 10^5$ and $F/F_0^{max} = 1.7 \pm 0.03$ for SGTx1; triangles for 100 mM K^+, 1 mM free Ca^{2+} data: $K_x = (4.8 \pm 0.01) \times 10^4$ and $F/F_0^{max} = 2.1 \pm 0.1$ for hanatoxin, and $K_x = (1.9 \pm 0.01) \times 10^4$ and $F/F_0^{max} = 2.0 \pm 0.5$ for SGTx1; closed circles for 100 mM K^+, 1 mM Ca^{2+}, 0.3 mM Mg^{2+}, pH 7.6 (PB). Data from Fig 2 (E and F) for HEB solution are shown for comparison using open circles. Stern-Volmer plots for acrylamide quenching of W30 fluorescence of hanatoxin (C and E) and SGTx1 (D and F) in physiological buffer (PB) (2 μM, black diamonds) and in the presence of either anionic (C and D) or neutral (E and F) lipid vesicles (0.9 mM, blue circles). In all cases data points are the mean ± SEM ($n = 3$). (G) Reversed-phase HPLC profiles of hanatoxin, SGTx, and agitoxin-2 present in the supernatant in the absence (black) or in the presence of 300 oocytes (blue) resuspended in physiological buffer (PB). The calculated fraction partitioned ($f_P = ([Toxin_{total}] - [Toxin_{free}])/[Toxin_{total}]$) is 0.31 ± 0.05 for hanatoxin, 0.25 ± 0.04 for SGTx1, and 0.01 ± 0.01 for agitoxin-2. Data are the mean ± SEM ($n = 3$). Traces were normalized to the maximum absorbance in the absence of oocytes.

tryptophan fluorescence to determine K_x values for the interaction of SGTx1 mutants with anionic vesicles, where the most accurate measurements of K_x can be obtained. Fig. 5 (A and B) shows example spectra in control aqueous solution and in the presence of a saturating concentration of lipid vesicles, and corresponding titration experiments for WT, D24A, and R3A SGTx1. In most instances, the strength of partitioning into model membranes is weakened by the mutation (e.g., R3A), while in others partitioning is strengthened (e.g., D24A) (Fig. 5, A–C; Table III). The K_x values for partitioning of all 24 mutants into anionic membranes are plotted in Fig. 5 C, and the changes in partitioning free energy ($\Delta\Delta G_P = -RT \ln K_x^{mut}/K_x^{WT}$) are mapped onto the NMR structure of SGTx1 in Fig. 5 D. There are two interesting observations that emerge from these data. First, the face of SGTx1 containing the hydrophobic protrusion and the C-terminal tail contain the most important determinants of toxin partitioning. Second, both hydrophobic and electrostatic interactions are important for the interaction of SGTx1 with anionic membranes. We also used the depletion assay described above for oocytes to examine how a select group of mutations influence partitioning into native membranes, including mutations that neutralize basic residues (R3A, R22A, K26A) or acidic residues (D24A, D31A), and those that truncate hydrophobic side chains (Y4A, L5A, F6A, W30A, F34A) (Fig. 5, E–G). Although a rigorous quantitative evaluation of these results is not possible given the qualitative nature of the oocyte assay, the results suggest that partitioning of toxins into native membranes relies more on hydrophobic interactions (Fig. 5, E and F). In contrast to the results with anionic membranes, the basic residue neutralizations do not significantly weaken toxin interactions with oocytes and the effects of the enhanced partitioning of the D24A mutation appear less significant (Fig. 5 G). These results are consistent with the notion that anionic lipids are scarce in the external leaflet of oocyte membranes and they are in agreement with the recent studies indicating a complex interplay between hydrophobic and electrostatic interactions between SGTx1 and model membranes (Posokhov et al., 2007b).

Mutations in specific regions of SGTx1 also have interesting effects on the spectral properties of the

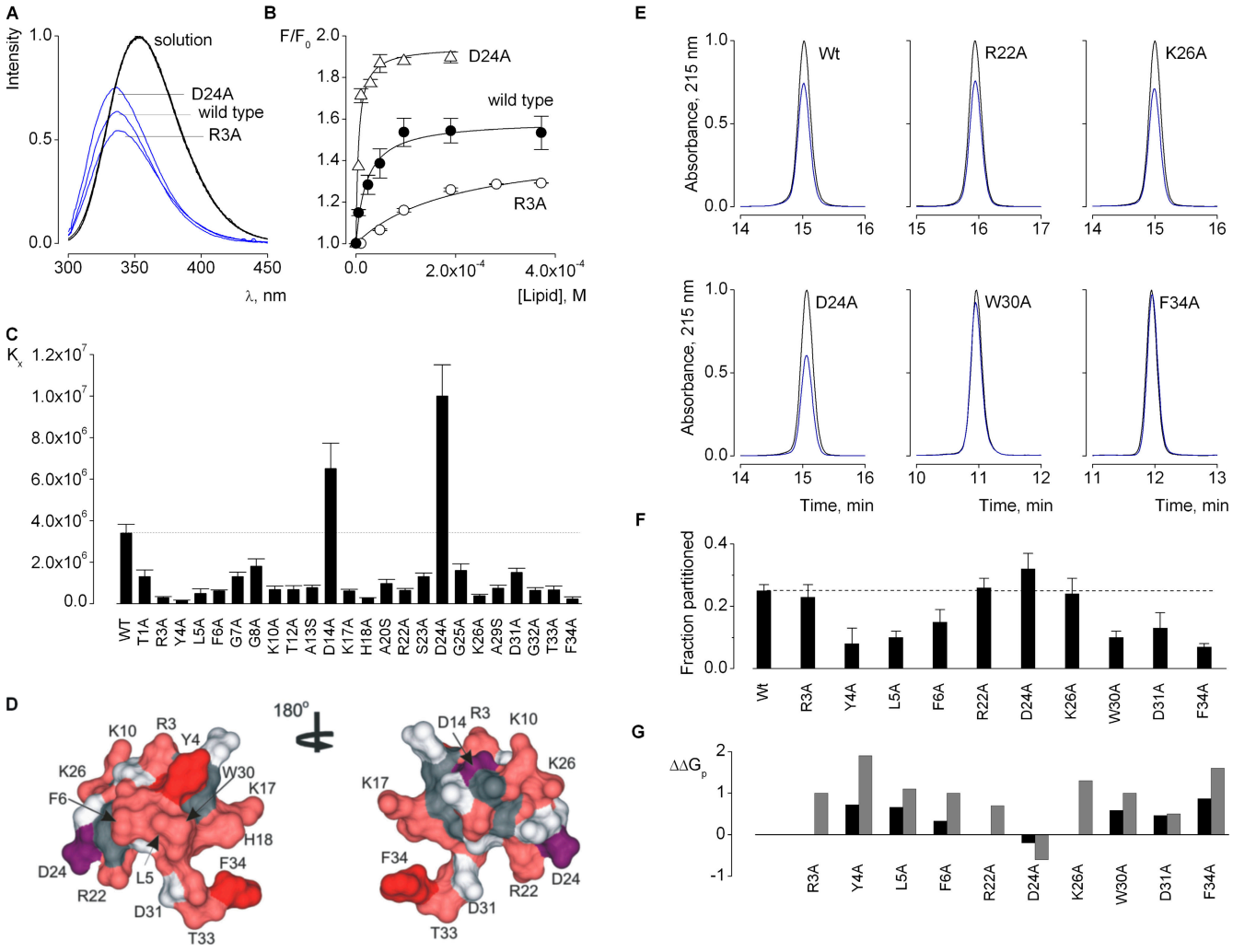

Figure 5. Effect of SGTx1 mutations on partitioning into membranes. (A) Toxins fluorescence spectra in the absence (black) or presence of anionic lipid vesicles (blue). The lipid concentration was 0.4 mM. (B) Fluorescence intensity at 320 nm for WT, D24A, and R3A plotted as a function of available lipid concentration (60%). Data points are the mean ± SEM ($n = 3$). Smooth curves are fits of a partition function to the data with the following parameters: $K_x = (1.0 \pm 0.03) \times 10^7$ and $F/F_0^{max} = 2.0 \pm 0.02$ for D24A (open triangles), and $K_x = (7.0 + 0.1) \times 10^5$ and $F/F_0^{max} = 1.4 \pm 0.03$ for R3A (open circles). Data for WT SGTx is shown for comparison (solid circles, same as in Fig. 2 F). (C) K_x values for partitioning of WT and mutant SGTx1 into anionic lipids. (D) Perturbations in partitioning into anionic membranes mapped onto the SGTx1 NMR solution structure, shown as a surface rendering with a probe radius of 1 Å. Side-chain colors are as follows: light gray for $|\Delta\Delta G_P| < 1$ kcal/mol, pink for $|\Delta\Delta G_P| = 1$–1.5 kcal/mol, red for $|\Delta\Delta G_P| > 1.5$ kcal/mol, and purple for $\Delta\Delta G_P < -1$ kcal/mol. Backbone and all other residues are colored dark gray. Structure in the right panel was rotated 180° about the indicated axis. Changes in free energy were calculated as: $\Delta\Delta G_P = -RT\ln(K_x^{mut}/K_x^{WT})$. The change in K_x value for W30A relative to WT ($\Delta\Delta G_P \sim 1$ kcal mol^{-1}) was estimated from depletion experiments. (E) Reversed-phase HPLC profiles of WT and mutant SGTx1 toxins present in the supernatant in the absence (black) or in the presence of 300 *X. laevis* oocytes (blue). Traces were normalized to the maximum in the absence of oocytes. (F) Fraction of toxin partitioned into oocytes membranes. Data are the mean ± SEM ($n = 3$). The dotted line corresponds to the value for wild type SGTx1. (G) Comparison between the effect of mutations on partitioning into model (gray, same as in C and D) and native membranes (black).

membrane-bound peptides. Whereas for all mutants examined, the spectra in aqueous solution were very similar, with λ_{max} values near 353 nm (Fig. 5 A; Fig. 6 A), we observe a relatively wide distribution of λ_{max} values in the presence of high lipid concentrations (Fig. 6 A), suggesting that W30 can be positioned in distinct microenvironments when the toxins are bound to membranes. The WT toxin and many of the mutants fall into the most blue-shifted end of the distribution, with λ_{max} values between 335 and 339 nm, consistent with the notion that W30 experiences a rather buried hydrophobic environment in these cases. The other end of the distribution consists of six mutants (F6A, H18A, D31A, G32A, T33A, and F34A) that have λ_{max} values between 341 and 349 nm, more typical of incompletely buried tryptophan residues in microenvironments that are partially exposed to bound water (Burstein et al., 2001; Reshetnyak and Burstein, 2001). These two groups of

TABLE III

Effects of SGTx Mutations on Interactions of the Toxin with Anionic Membranes

SGTx1	K_x	$\Delta\Delta G_P$	$\Delta\Delta G_O$
		kcal mol^{-1}	*kcal mol*$^{-1}$
WT	3.4×10^6	–	–
T1A	1.3×10^6	0.6	0.0
R3A	7.0×10^5	1.0	>3.0
Y4A	1.5×10^5	1.9	1.2
L5A	4.9×10^5	1.1	>3.0
F6A	6.1×10^5	1.0	>3.4
G7A	1.3×10^6	0.6	0.8
G8A	1.8×10^6	0.4	0.2
K10A	6.8×10^5	1.0	0.4
T12A	6.8×10^5	1.0	0.2
A13S	7.7×10^5	0.9	0.1
D14A	6.5×10^6	−0.4	−1.1
K17A	6.1×10^5	1.0	0.3
H18A	2.7×10^5	1.5	1.2
A20S	9.7×10^5	0.7	0.7
R22A	7.9×10^5	0.7	>3.0
S23A	1.3×10^6	0.6	0.4
D24A	1.0×10^7	−0.6	−1.8
G25A	1.6×10^6	0.4	0.4
K26A	3.9×10^5	1.3	0.5
A29S	7.4×10^5	0.9	1.2
D31A	1.5×10^6	0.5	1.4
G32A	6.4×10^5	1.0	0.8
T33A	6.7×10^5	1.0	0.8
F34A	2.3×10^5	1.6	0.7

$\Delta\Delta G_O$ values are from Wang et al. (2004).

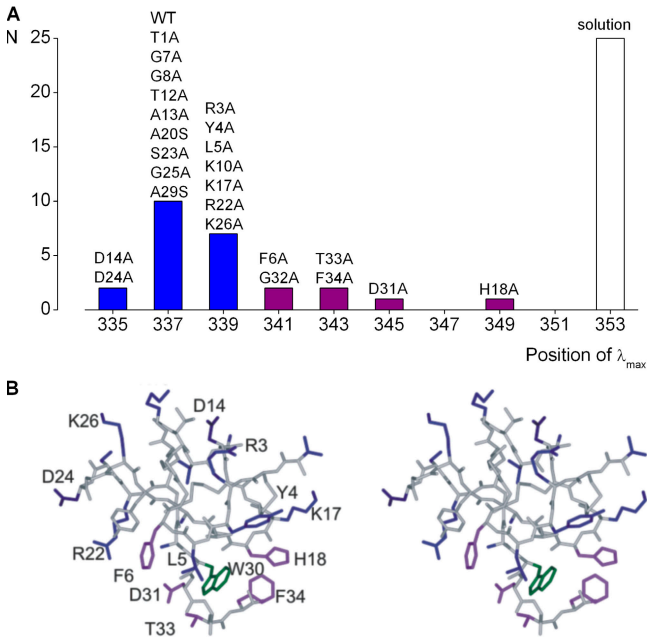

Figure 6. Spectral characteristics of SGTx1 peptides. (A) λ_{max} for WT and SGTx1 mutants free in solution (open bar) or in the presence of 2.4 mM anionic liposomes (blue for λ_{max} values within 2 nm of that observed for WT and purple for all others). (B) Spectral characteristics of membrane-bound toxins mapped onto the NMR solution structure of SGTx1. Side-chain colors for the stereo pairs are as follows: blue for WT-like spectra, purple for red-shifted maxima, and green for W30. All other side chains and backbone are gray.

mutants are segregated in an intriguing fashion in the structure of SGTx1, with those that perturb the environment of W30 (purple residues) clustered on one side of the toxin near W30, and those that don't (blue residues) on the other side of the toxin (Fig. 6 B). Presumably those mutants that perturb the membrane environment of W30 cause the toxin to adopt a somewhat different position within the membrane, changing either the depth or orientation of the toxin to expose W30 to water within the headgroup layer. This possibility is supported by acrylamide-quenching experiments on membrane-bound H18A SGTx1, which reveal greatly increased accessibility of W30 to aqueous acrylamide (unpublished data). Interestingly, the mutations that perturb the microenvironment of W30 partially overlap with those that perturb the strength of partitioning (compare Fig. 5 D and Fig. 6 B), suggesting that this region is crucial for both the position and stability of the toxin in lipid membranes.

Toxin Stereoselectivity

It is well established that amphipathic molecules alter the mechanical properties of lipid bilayers (Lundbaek and Andersen, 1994; Andersen et al., 1999), and one might predict that hanatoxin and SGTx1 would have significant effects on membrane properties. GsMTx-4 is a related tarantula toxin that inhibits stretch-activated cation channels, and it has been shown that both D and L enantiomers are active, suggesting that the toxin inhibits the channel through a perturbation of the bilayer rather than through a direct toxin–channel interaction (Suchyna et al., 2004). Although mutations in the paddle can disrupt the inhibitory effects of hanatoxin (Swartz and MacKinnon, 1997b; Li-Smerin and Swartz, 2000, 2001; Phillips et al., 2005), it is possible that these channel residues detect toxin-induced bilayer perturbations rather than taking part in a protein–protein interaction. This a reasonable possibility considering that partitioning under physiologically relevant conditions ($Kx \sim 10^3$) would be expected to result in a toxin:lipid ratio in the outer leaflet of ~1:10,000, which means that the toxin concentration in the outer leaflet could be as much as 1,000-fold higher than the water phase. To investigate whether tarantula toxins might inhibit K_v channels indirectly without binding the channel, we synthesized the D-enantiomer of SGTx1, which should influence bilayer properties similarly to the L-enantiomer given the fluid nature of the lipid membrane, but should not participate in a protein–protein interaction. The D and L enantiomers have identical reverse-phase HPLC profiles (Fig. 7 A) and similar secondary structure

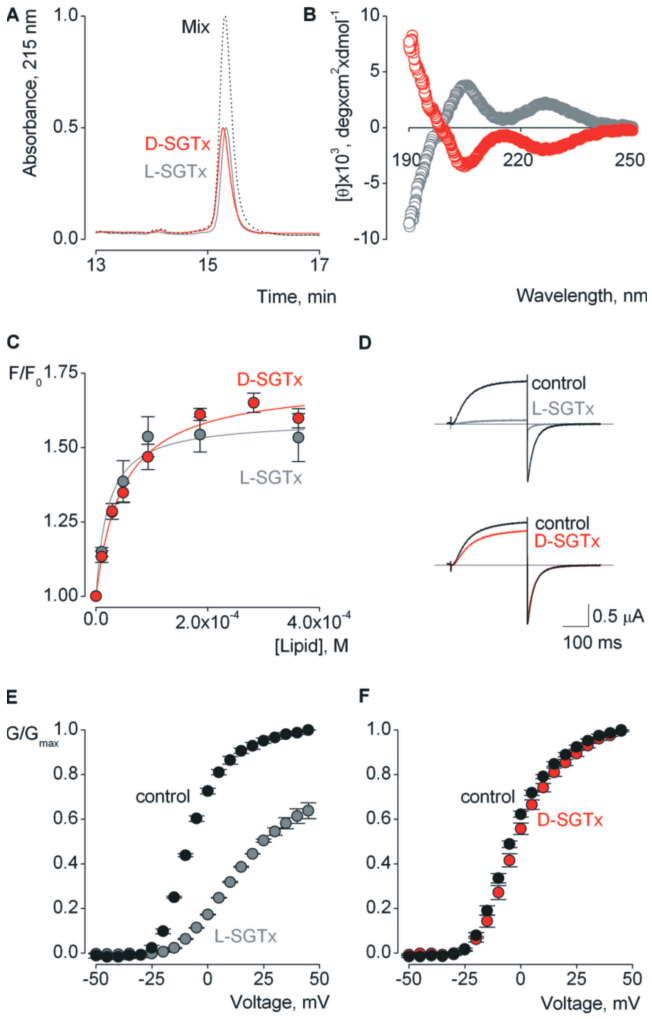

Figure 7. Comparison of the biochemical and functional behavior of SGTx1 enantiomers. (A) Reversed-phase HPLC profiles of L-SGTx (gray) and D-SGTx (red) injected either separately or together (dotted black trace). (B) Circular dichroism spectra of L-SGTx (gray symbols) and D-SGTx (red symbols). (C) Fluorescence intensity at 320 nm plotted as a function of available lipid concentration (60%) for a 1:1 mix of POPC: POPG. Smooth red curve is the fit to the D-SGTx data and corresponds to a partition function with $K_x = (1.2 \pm 0.2) \times 10^6$ and $F/F_0^{max} = 1.7 \pm 0.03$. Data for L-SGTx is shown for comparison (gray, same as in Fig. 2 F). (D) Voltage-clamp recording from an oocyte expressing the $K_v2.1$ channel. Currents were elicited by depolarization to −10 mV in the absence (black) or presence of 8 μM L-SGTx1 (gray) or 8 μM D-SGTx1 (red). The holding voltage was −100 mV, and the tail voltage was −50 mV. The light gray line indicates the level of zero current. Leak, background, and capacitive currents were subtracted after blocking the channel with agitoxin-2. Voltage–activation relations in the absence (black) and presence of 8 μM L-SGTx1 (gray) (E) or 8 μM D-SGTx1 (red) (F). Tail currents obtained following depolarizations were averaged for 0.2 ms beginning 2 ms after repolarization to −50 mV. In all case data points are the mean ± SEM ($n = 3$).

as shown by CD spectroscopy (Fig. 7 B). As expected, the CD spectra nicely illustrate that the two enantiomers are mirror images. Examination of the strength of membrane partitioning using intrinsic tryptophan fluorescence shows that D-SGTx partitions into anionic membranes with a K_x of $(1.2 \pm 0.2) \times 10^6$ (Fig. 7 C), similar to the value of 3.4×10^6 obtained for the L-enantiomer under identical conditions. In control experiments, addition of L-SGTx1 to the extracellular solution produces nearly complete inhibition of macroscopic K_v channel currents when activating the channel with weak depolarizations (Fig. 7 D, top), and shifts channel activation to more depolarized voltages (Fig. 7 E), in agreement with previous reports (Lee et al., 2004; Wang et al., 2004). In contrast, the change in K_v channel current observed upon addition of D-SGTx is quite small (Fig. 7 D) and the voltage dependence of the channel activation is similar to that in the absence of toxin (Fig. 7 F). Although it is possible that the small effects observed with the D-enantiomer reflect a change in membrane properties, the pronounced inhibitory effects of the L-enantiomer are not observed with the D-enantiomer, suggesting that partitioning of the toxin into the membrane is not sufficient to modify the gating of K_v channels. We conclude that the mechanism of inhibition must involve direct toxin–channel interactions.

Region of Tarantula Toxins Interacting with Paddle Motifs

The effects of SGTx1 mutations on the apparent affinity of the toxin have been previously assessed from experiments in which the aqueous concentration of the toxin is varied and the resulting changes in toxin occupancy of the channel determined (Wang et al., 2004). If tarantula toxins interact with paddle motifs within the membrane, toxin mutations might perturb the apparent K_d through several mechanisms, including (a) perturbing the strength of toxin partitioning into the bulk membrane, which would alter the concentration of the toxin in the membrane, (b) altering the interaction between the toxin and the membrane in the toxin–channel complex, which could influence the stability of the complex, and (c) perturbing protein–protein interactions between the toxin and the channel. Although mutants might have rather complex effects through these mechanisms, those that disproportionately perturb the apparent affinity relative to membrane partitioning would likely do so by altering the strength of the protein–protein interaction. To look for mutations of this type we plotted the change in partitioning free energy estimated from K_x values ($\Delta\Delta G_P = -RT \ln K_x^{mut}/K_x^{WT}$) against the change in overall free energy estimated from apparent K_d values ($\Delta\Delta G_O = -RT \ln K_d^{mut}/K_d^{WT}$) (Wang et al., 2004) (Fig. 8 A). Although there appears to be a loose relationship between $\Delta\Delta G_P$ and $\Delta\Delta G_O$, the two quantities do not tightly correlate, and in general the perturbations in the toxin–membrane interaction are relatively modest ($|\Delta\Delta G_P| < 2$ kcal mol^{-1}) compared with those for the overall energetics, which can exhibit $\Delta\Delta G_O$ values >3.4 kcal mol^{-1} (Fig. 8 A). In particular, one group of mutations, including R3A, L5A, F6A, R22A,

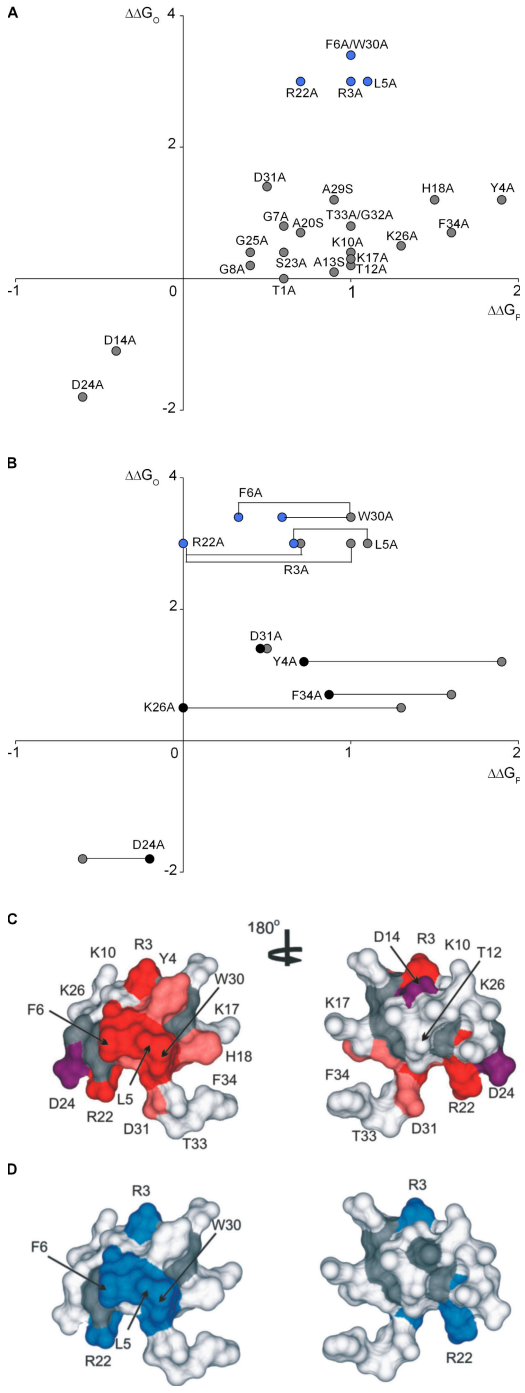

Figure 8. Comparison of the effects of SGTx1 mutations on membrane partitioning and apparent affinity. (A) Perturbations in toxin partitioning into model membranes ($\Delta\Delta G_P$) from Fig. 5, C and D, plotted against changes in apparent toxin affinity for $K_v2.1$ channels ($\Delta\Delta G_O$). Blue symbols indicate the values for residues proposed to be involved in direct toxin–channel interactions. $\Delta\Delta G_O = -RT\ln(K_d^{mut}/K_d^{WT})$, where K_d is the apparent equilibrium dissociation constant determined from experiments in which aqueous toxin concentration is varied and the resulting fraction of unbound channels measured when activating the channel using weak depolarizations (Swartz and MacKinnon, 1997a). Apparent K_d values are from Wang et al. (2004). (B) Perturbations in toxin partitioning into native membranes ($\Delta\Delta G_P$) from Fig. 5 G plotted against changes in apparent toxin affinity for $K_v2.1$ channels ($\Delta\Delta G_O$). Data from A is shown for comparison (gray). (C) Perturbations in apparent K_d mapped onto the SGTx1 NMR solution structure, shown as a surface rendering with a probe radius of 1 Å. Side-chain colors are as follows: light gray for $|\Delta\Delta G_O| < 1$ kcal/mol, pink for $|\Delta\Delta G_O| = 1$–1.5 kcal/mol, red for $|\Delta\Delta G_O| > 1.5$ kcal/mol, and purple for $\Delta\Delta G_O < -1$ kcal/mol. Backbone and all other residues are colored dark gray (Wang et al., 2004). (D) Residues proposed to participate in direct toxin–channel interaction are colored blue, all other residues studied are colored white, backbone and unstudied residues are colored dark gray. In the right panels the structures were rotated 180° about the indicated axis.

and W30, produce much larger perturbations of the apparent K_d compared with the toxin–membrane interaction (Fig. 8 A). The disproportionate perturbation in apparent affinity relative to membrane partitioning is even more pronounced if perturbations in toxin–membrane interactions are assessed using the depletion assay described above for oocyte membranes (Fig. 8 B). Importantly, residues in this group form a cluster on a single face of the toxins (Fig. 8, C and D), thus identifying the region of the toxin that likely participates in a direct protein–protein interaction with the paddle motif (Fig. 8 D).

Membrane Modification Alters Toxin Inhibition

The results thus far shed light on the interaction of tarantula toxins with membranes of varying composition, define the regions of the toxin that are important for interacting with membranes, and constrain regions that are important for binding to voltage-sensor paddle motifs. To look for evidence that the toxin–channel interaction actually occurs within the membrane we examined whether biochemical modification of the lipid bilayer influences the interaction of tarantula toxins with the $K_v2.1$ channel. Recent results from Lu and colleagues (Ramu et al., 2006) show that treatment of oocytes with SMaseD, an enzyme that converts the zwitterionic lipid sphingomyelin (SM) to the anionic ceramide-1-phosphate (C-1-P), shifts activation of $K_v2.1$ by ~30 mV. Following enzyme treatment, the Kv2.1 channel retains sensitivity to hanatoxin (Ramu et al., 2006), although the apparent kinetics of the toxin–channel interaction are altered (Ramu, Y., and Lu, Z., personal communication). In control experiments the addition of hanatoxin to the extracellular solution inhibits activation of $K_v2.1$ by shifting activation to more depolarized voltages (Fig. 9, A and B), and channel activity recovers very slowly upon removal of the toxin from the aqueous solution, requiring ~1,000 s to reach control values. Kinetic analysis of mutations within the voltage-sensor paddle suggest that slow recovery results from slow unbinding of the toxin, with a dwell time of several hundred seconds (Phillips et al., 2005). In contrast to what is observed under control conditions, the kinetics for both the onset and recovery from inhibition by hanatoxin are

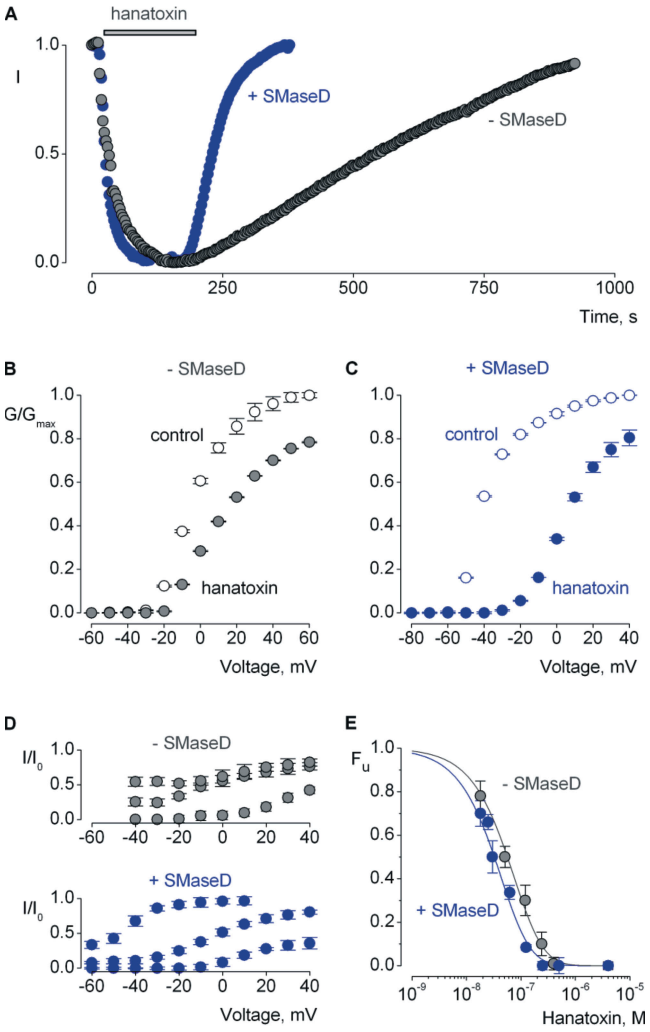

Figure 9. Effect of sphingomyelinase D on inhibition of $K_v2.1$ channels by hanatoxin. (A) Time course for effects of hanatoxin (500 nM) on the $K_v2.1$ channel before (gray) and after 15 min treatment of oocytes with SMaseD (blue). I is tail current amplitude at −80 mV elicited following depolarizations to −10 mV for control (gray) or −50 mV after SMaseD treatment (blue), normalized to the value in the absence of toxin. Voltage–activation relations for $K_v2.1$ before (B) or after SMaseD treatment (C) in the absence (open symbols) or presence (solid symbols) of 100 nM hanatoxin. Tail currents obtained following depolarizations were averaged for 0.2 ms beginning 2 ms after repolarization to −80 mV. (D) Fraction of uninhibited current plotted against test voltage at three hanatoxin concentrations (50 nM, 100 nM, 4 μM) for untreated (top, gray) and SMaseD-treated (bottom, blue) oocytes. (E) Concentration dependence for inhibition of $K_v2.1$ channel. F_u, the fraction of unbound channels, was estimated from fractional inhibition at negative voltages (Swartz and MacKinnon, 1997a; Phillips et al., 2005). Smooth curves are fits of $F_u = (1 - P)^4$ where $P = [\text{Toxin}]/([\text{Toxin}] + K_d)$ with $K_d = 298 \pm 14$ nM for unmodified membranes (gray), and $K_d = 170 \pm 10$ nM after SMaseD treatment (blue). Leak, background, and capacitive currents were subtracted after blocking the channel with agitoxin-2. In all case data points are the mean ± SEM ($n = 3$).

dramatically altered following treatment with SMaseD (Fig. 9 A). In particular, recovery of channel activity occurs quite rapidly, requiring little more than 100 s to reach control values. These results suggest that modification of SM speeds dissociation of the toxin by weakening the toxin–channel interaction, as observed with mutations in the paddle motif (Phillips et al., 2005). However, rather counter intuitively, comparison of the concentration dependence for toxin occupancy of the channel reveals that SMaseD treatment does not shift the apparent K_d to higher toxin concentrations, and in fact produces a modest shift of the relation to lower toxin concentrations (Fig. 9, D and E). The most straightforward interpretation of these results is that SM interacts intimately with the channel in the local vicinity of where the toxin binds and that hydrolysis of the lipid weakens the toxin–channel interaction. The pronounced effects of anionic lipids on toxin partitioning (Figs. 2–4) can explain why the apparent affinity doesn't decrease, because the anionic product of SMase action (C-1-P) would be expected to increase the concentration of the toxin in the membrane. We do not observe an increase in hanatoxin partitioning into bulk *Xenopus laevis* oocyte membranes after SMaseD treatment (unpublished data), suggesting that the increase in toxin concentration may only occur in the local vicinity of the channel. Regardless of the actual mechanism, the opposing effects of SMaseD on the kinetics of recovery and the apparent K_d strongly suggest that the toxin and the channel interact within the lipid membrane. The destabilizing effect of SMaseD on the toxin–channel interaction supports the proposal that SM interacts relatively specifically with certain K_v channels (Ramu et al., 2006).

DISCUSSION

The objective of the present study was to characterize the interaction of voltage-sensor toxins with membranes, and to explore whether membrane partitioning is involved in the mechanism by which these toxins inhibit K_v channels. Our experiments with model membranes demonstrate that the strength of partitioning depends on the type of lipids and the ionic composition of the aqueous solution. Partitioning is most favorable in the presence of anionic lipids, where electrostatic interactions help to stabilize the toxin in the membrane (Figs. 2–5), but significant partitioning into zwitterionic membranes can be observed even in the presence of physiological aqueous solutions (Fig. 4). Since anionic lipids are relatively scarce in the outer leaflet of native membranes (Simons and van Meer, 1988; Calderon and DeVries, 1997; Hill et al., 2005), partitioning into native membranes should be most similar to what we observed for zwitterionic model membranes. Our depletion experiments with whole oocytes are fully compatible with measurements on zwitterionic model membranes (Fig. 4),

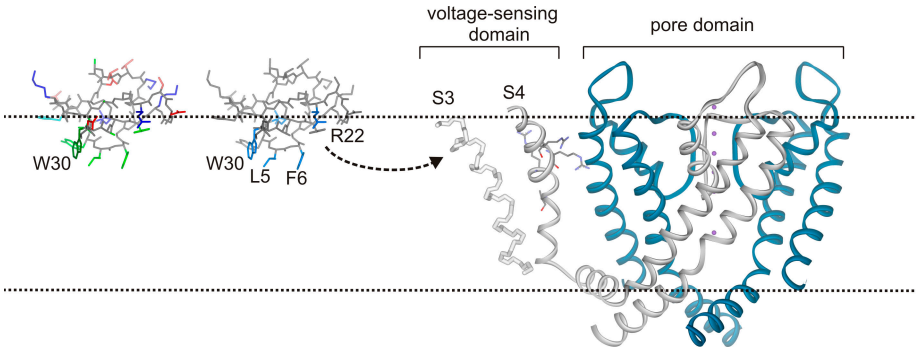

Figure 10. Interaction of tarantula toxins with voltage-sensor paddles within the membrane. Illustration of SGTx1 partitioning into the membrane and interacting with S3–S4 helices. Side chain colors for left SGTx1 structure are green for hydrophobic, blue for basic, red for acidic, pink for Ser/Thr, and gray for other side chains and backbone atoms. Right SGTx1 structure shows residues important for protein–protein interactions in light blue. In both cases G32-F34 have been removed for clarity. Backbone fold of the activated/open conformation of the $K_v1.2$ (protein database accession code2A79) shown with only one of four voltage-sensing domains. Side chains of the outer four S4 Arg residues are shown and both S1 and S2 helices have been deleted for clarity. The contribution of the back subunit to the pore domain has also been omitted for clarity. Purple spheres are positions of potassium ions within the ion conduction pathway.

both of which indicate that tarantula toxins can partition into native cell membranes with a K_x of $\sim 10^3$.

The evidence that voltage-sensor toxins can partition into membranes under physiological conditions raises the possibility that partitioning of these toxins may be sufficient to inhibit K_v channels. Perhaps these channels are sensitive to the properties of the bilayer, and the observed inhibitory effects result from indirect perturbations that occur without the toxin actually binding to the channel. We explored this possibility by synthesizing and studying the D-enantiomer of SGTx1, which would be expected to inhibit activation of the $K_v2.1$ channel if the mechanism involves a perturbation of the bilayer without the toxin actually binding to the channel. Although the D and L enantiomers interact with membranes in an indistinguishable fashion, D-SGTx1 is essentially inactive on the $K_v2.1$ channel (Fig. 7), indicating that direct protein–protein interactions are indeed involved in the inhibitory mechanism of the toxin.

The present results also substantially refine of our understanding of which toxin residues are involved in forming the complex between toxin and paddle. Although a previous study identified the face of the toxin that is crucial for inhibitory activity (Wang et al., 2004), toxin mutations that affect the apparent affinity could do so by perturbing both toxin–membrane and toxin–channel interactions. The present results suggest that the toxin side of the protein–protein interface likely involves R3, L5, F6, R22, and W30, which stand out in the plot of $\Delta\Delta G_P$ vs. $\Delta\Delta G_O$ because their mutation weakens toxin–membrane interactions rather modestly ($\Delta\Delta G_P < 1.1$ kcal mol^{-1}) compared with the apparent affinity ($\Delta\Delta G_O > 3$ kcal mol^{-1}; Fig. 8). The three hydrophobic residues in the group of outliers (L5, F6, and W30) are tightly packed together on one face of the toxin, with the two basic residues (R3, R22) positioned nearby in the surrounding ring of polar residues, constraining the surface of the toxin that participates in protein–protein interactions with the voltage-sensor paddle (Fig. 8 D). This picture is consistent with mutagenesis studies on $K_v2.1$, which have identified a glutamate and several hydrophobic residues in S3b of the paddle motif that are critical for interacting with tarantula toxins (Swartz and MacKinnon, 1997b; Li-Smerin and Swartz, 2000, 2001).

The ability of tarantula toxins to partition into membranes implies that the targeted paddle motif could be submerged in the membrane, but also that the toxin concentration in the membrane could be considerably higher than in the aqueous solution. For example, if a toxin partitions with a K_x of 10^6, the effective membrane concentration could be as much as 10^5-fold higher, allowing a very weak (e.g., mM) protein–protein interaction to achieve apparent high affinity (e.g., nM) (Lee and MacKinnon, 2004). Although the relative energetic contributions of protein–protein and protein–lipid interactions will likely vary for each toxin–channel pair studied in different membrane environments, the interaction of the present toxins with $K_v2.1$ in native membranes is probably somewhere in the middle of the spectrum, with both types of interactions playing important roles. The importance of the protein–protein interface is supported by the observation that in most cases the relatively subtle effects of SGTx1 mutations on the free energy of partitioning cannot account for their effects on the concentration dependence for toxin occupancy of the channel (Fig. 8). That $\Delta\Delta G_O$ values cannot be explained by $\Delta\Delta G_P$ values alone is perhaps most clearly seen for two Phe to Ala mutants. The $\Delta\Delta G_P$ values for F6A and F34A are similar, with that for F34A being somewhat greater, yet the values for $\Delta\Delta G_O$ are vastly different, with that for F6A being far greater compared with F34A (Figs. 5 and 8; Table III). In addition, the effects of paddle mutations on recovery kinetics suggest that the toxin remains bound to the channel for hundreds of seconds (Phillips et al., 2005), pointing to a rather stable toxin–channel complex. The importance of the toxin–membrane interaction is highlighted by the estimated K_x values of 10^3 for hanatoxin and SGTx1 partitioning into membranes

under physiological conditions. Although these values are much lower than those observed for anionic membranes, they are sufficient to raise the toxin concentration in the membrane considerably compared with the aqueous phase. The relative contributions of the partitioning step may be even more significant for the interaction of VSTx1 with K_vAP channels studied in anionic membranes, where the K_x is $\sim 10^5$, the affinity of the protein–protein interaction is in the mM range, yet nM concentrations of the toxin produce robust inhibition (Lee and MacKinnon, 2004). The interaction of scorpion toxins with Na_v channels may be an example where protein–protein interactions are even more dominant than what we have observed for hanatoxin and SGTx1. It is important to note that the high-affinity binding of scorpion toxins to Na_v channels (Rogers et al., 1996; Cohen et al., 2006), however, does not rule out the possibility that partitioning may be required for toxin binding to the voltage sensors in those channels (Smith et al., 2005). It would be difficult to convincingly demonstrate partitioning if the K_x values were much less than 10^3, yet even a K_x of 10^2 would suggest that membrane concentrations of the toxin are somewhat higher than in the bulk aqueous phase, more than adequate for a toxin to access its receptor within the membrane. Similarly, the failure to observe an interaction of tarantula toxins like HpTx2 with zwitterionic membranes at physiological pH (Posokhov et al., 2007b) does not preclude the involvement of membrane partitioning for inhibition of Kv4 channels because the methods used are not sensitive enough to detect partitioning with a K_x value of 10^2.

Our working model for the interaction of tarantula toxins with K_v channels is illustrated in Fig. 10, where SGTx1 is shown interacting with the voltage-sensor paddle within the membrane. Although many of our findings are consistent with toxin–channel interactions occurring within the bilayer, perhaps the strongest evidence to support this idea comes from the effects of SMaseD on inhibition by hanatoxin. The effects of this lipase on the recovery from inhibition show that the stability of the toxin–channel complex is remarkably sensitive to modification of the lipid environment (Fig. 9). Conversion of SM to C-1-P dramatically speeds dissociation of the toxin, suggesting that SM interacts intimately with the channel in such a way that it influences the toxin–channel interaction. It is as if the lipid, channel, and toxin form a trimolecular complex, and that relatively subtle changes in the lipid molecule can be readily detected by the toxin. Although there is much to learn about the interaction between these three types of molecules, the emerging picture strongly suggests that the voltage-sensor paddle motif moves at the interface where the channel meets the surrounding lipid membrane (Jiang et al., 2003a,b; Ruta et al., 2003, 2005; Cuello et al., 2004; Lee et al., 2005; Schmidt et al., 2006).

We thank Lorin Milescu, Joseph Mindell, Shai Silberberg, and members of the Swartz lab for helpful discussions, Dmitriy Krepkiy for assistance with collection of CD spectra, and Zhe Lu (University of Pennsylvania, Philadelphia, PA) for generously providing SMaseD.

This work was supported by the Intramural Research Program of the National Institute of Neurological Disorders and Stroke, National Institutes of Health.

Lawrence G. Palmer served as editor.

Submitted: 9 August 2007
Accepted: 27 September 2007

REFERENCES

Ahern, C.A., and R. Horn. 2004. Stirring up controversy with a voltage sensor paddle. *Trends Neurosci.* 27:303–307.

Andersen, O.S., C. Nielsen, A.M. Maer, J.A. Lundbaek, M. Goulian, and R.E. Koeppe II. 1999. Ion channels as tools to monitor lipid bilayer-membrane protein interactions: gramicidin channels as molecular force transducers. *Methods Enzymol.* 294:208–224.

Bemporad, D., Z.A. Sands, C.L. Wee, A. Grottesi, and M.S. Sansom. 2006. Vstx1, a modifier of Kv channel gating, localizes to the interfacial region of lipid bilayers. *Biochemistry.* 45:11844–11855.

Beschiaschvili, G., and J. Seelig. 1990. Melittin binding to mixed phosphatidylglycerol/phosphatidylcholine membranes. *Biochemistry.* 29:52–58.

Burstein, E.A., S.M. Abornev, and Y.K. Reshetnyak. 2001. Decomposition of protein tryptophan fluorescence spectra into log-normal components. I. Decomposition algorithms. *Biophys. J.* 81:1699–1709.

Calderon, R.O., and G.H. DeVries. 1997. Lipid composition and phospholipid asymmetry of membranes from a Schwann cell line. *J. Neurosci. Res.* 49:372–380.

Cestele, S., Y. Qu, J.C. Rogers, H. Rochat, T. Scheuer, and W.A. Catterall. 1998. Voltage sensor-trapping: enhanced activation of sodium channels by β-scorpion toxin bound to the S3-S4 loop in domain II. *Neuron.* 21:919–931.

Cestele, S., V. Yarov-Yarovoy, Y. Qu, F. Sampieri, T. Scheuer, and W.A. Catterall. 2006. Structure and function of the voltage sensor of sodium channels probed by a β-scorpion toxin. *J. Biol. Chem.* 281:21332–21344.

Cohen, L., N. Gilles, I. Karbat, N. Ilan, D. Gordon, and M. Gurevitz. 2006. Direct evidence that receptor site-4 of sodium channel gating modifiers is not dipped in the phospholipid bilayer of neuronal membranes. *J. Biol. Chem.* 281:20673–20679.

Cuello, L.G., D.M. Cortes, and E. Perozo. 2004. Molecular architecture of the KvAP voltage-dependent K^+ channel in a lipid bilayer. *Science.* 306:491–495.

Doyle, D.A., J. Morais Cabral, R.A. Pfuetzner, A. Kuo, J.M. Gulbis, S.L. Cohen, B.T. Chait, and R. MacKinnon. 1998. The structure of the potassium channel: molecular basis of K^+ conduction and selectivity. *Science.* 280:69–77.

Garcia, M.L., M. Garcia-Calvo, P. Hidalgo, A. Lee, and R. MacKinnon. 1994. Purification and characterization of three inhibitors of voltage-dependent K^+ channels from Leiurus quinquestriatus var. hebraeus venom. *Biochemistry.* 33:6834–6839.

Gill, S.C., and P.H. von Hippel. 1989. Calculation of protein extinction coefficients from amino acid sequence data. *Anal. Biochem.* 182:319–326.

Hill, W.G., N.M. Southern, B. MacIver, E. Potter, G. Apodaca, C.P. Smith, and M.L. Zeidel. 2005. Isolation and characterization of the *Xenopus* oocyte plasma membrane: a new method for studying activity of water and solute transporters. *Am. J. Physiol. Renal Physiol.* 289:F217–F224.

Jiang, Y., A. Lee, J. Chen, V. Ruta, M. Cadene, B.T. Chait, and R. MacKinnon. 2003a. X-ray structure of a voltage-dependent K+ channel. *Nature.* 423:33–41.

Jiang, Y., V. Ruta, J. Chen, A. Lee, and R. MacKinnon. 2003b. The principle of gating charge movement in a voltage-dependent K^+ channel. *Nature.* 423:42–48.

Jung, H.J., J.Y. Lee, S.H. Kim, Y.J. Eu, S.Y. Shin, M. Milescu, K.J. Swartz, and J.I. Kim. 2005. Solution structure and lipid membrane partitioning of VSTx1, an inhibitor of the KvAP potassium channel. *Biochemistry.* 44:6015–6023.

Kubo, Y., T.J. Baldwin, Y.N. Jan, and L.Y. Jan. 1993. Primary structure and functional expression of a mouse inward rectifier potassium channel. *Nature.* 362:127–133.

Ladokhin, A.S., S. Jayasinghe, and S.H. White. 2000. How to measure and analyze tryptophan fluorescence in membranes properly, and why bother? *Anal. Biochem.* 285:235–245.

Lee, C.W., S. Kim, S.H. Roh, H. Endoh, Y. Kodera, T. Maeda, T. Kohno, J.M. Wang, K.J. Swartz, and J.I. Kim. 2004. Solution structure and functional characterization of SGTx1, a modifier of Kv2.1 channel gating. *Biochemistry.* 43:890–897.

Lee, H.C., J.M. Wang, and K.J. Swartz. 2003. Interaction between extracellular Hanatoxin and the resting conformation of the voltage-sensor paddle in Kv channels. *Neuron.* 40:527–536.

Lee, S.Y., and R. MacKinnon. 2004. A membrane-access mechanism of ion channel inhibition by voltage sensor toxins from spider venom. *Nature.* 430:232–235.

Lee, S.Y., A. Lee, J. Chen, and R. Mackinnon. 2005. Structure of the KvAP voltage-dependent K^+ channel and its dependence on the lipid membrane. *Proc. Natl. Acad. Sci. USA.* 102:15441–15446.

Li-Smerin, Y., and K.J. Swartz. 1998. Gating modifier toxins reveal a conserved structural motif in voltage-gated Ca^{2+} and K^+ channels. *Proc. Natl. Acad. Sci. USA.* 95:8585–8589.

Li-Smerin, Y., and K.J. Swartz. 2000. Localization and molecular determinants of the Hanatoxin receptors on the voltage-sensing domains of a K^+ channel. *J. Gen. Physiol.* 115:673–684.

Li-Smerin, Y., and K.J. Swartz. 2001. Helical structure of the COOH terminus of S3 and its contribution to the gating modifier toxin receptor in voltage-gated ion channels. *J. Gen. Physiol.* 117:205–218.

Long, S.B., E.B. Campbell, and R. Mackinnon. 2005. Crystal structure of a mammalian voltage-dependent *Shaker* family K^+ channel. *Science.* 309:897–903.

Lu, Z., A.M. Klem, and Y. Ramu. 2001. Ion conduction pore is conserved among potassium channels. *Nature.* 413:809–813.

Lundbaek, J.A., and O.S. Andersen. 1994. Lysophospholipids modulate channel function by altering the mechanical properties of lipid bilayers. *J. Gen. Physiol.* 104:645–673.

Miller, C. 1995. The charybdotoxin family of K^+ channel-blocking peptides. *Neuron.* 15:5–10.

Nagle, J.F., and S. Tristram-Nagle. 2000. Structure of lipid bilayers. *Biochim. Biophys. Acta.* 1469:159–195.

Patton, C., S. Thompson, and D. Epel. 2004. Some precautions in using chelators to buffer metals in biological solutions. *Cell Calcium.* 35:427–431.

Phillips, L.R., M. Milescu, Y. Li-Smerin, J.A. Mindell, J.I. Kim, and K.J. Swartz. 2005. Voltage-sensor activation with a tarantula toxin as cargo. *Nature.* 436:857–860.

Polozov, I.V., A.I. Polozova, V.K. Mishra, G.M. Anantharamaiah, J.P. Segrest, and R.M. Epand. 1998. Studies of kinetics and equilibrium membrane binding of class A and class L model amphipathic peptides. *Biochim. Biophys. Acta.* 1368:343–354.

Posokhov, Y.O., P.A. Gottlieb, and A.S. Ladokhin. 2007a. Quenching-enhanced fluorescence titration protocol for accurate determination of free energy of membrane binding. *Anal. Biochem.* 362:290–292.

Posokhov, Y.O., P.A. Gottlieb, M.J. Morales, F. Sachs, and A.S. Ladokhin. 2007b. Is lipid bilayer binding a common property of inhibitor cysteine knot ion-channel blockers? *Biophys. J.* 93: L20–L22.

Ramu, Y., Y. Xu, and Z. Lu. 2006. Enzymatic activation of voltage-gated potassium channels. *Nature.* 442:696–699.

Reshetnyak, Y.K., and E.A. Burstein. 2001. Decomposition of protein tryptophan fluorescence spectra into log-normal components. II. The statistical proof of discreteness of tryptophan classes in proteins. *Biophys. J.* 81:1710–1734.

Rogers, J.C., Y. Qu, T.N. Tanada, T. Scheuer, and W.A. Catterall. 1996. Molecular determinants of high affinity binding of α-scorpion toxin and sea anemone toxin in the S3-S4 extracellular loop in domain IV of the Na^+ channel α subunit. *J. Biol. Chem.* 271:15950–15962.

Ruta, V., Y. Jiang, A. Lee, J. Chen, and R. MacKinnon. 2003. Functional analysis of an archaebacterial voltage-dependent K^+ channel. *Nature.* 422:180–185.

Ruta, V., J. Chen, and R. MacKinnon. 2005. Calibrated measurement of gating-charge arginine displacement in the KvAP voltage-dependent K^+ channel. *Cell.* 123:463–475.

Schmidt, D., Q.X. Jiang, and R. MacKinnon. 2006. Phospholipids and the origin of cationic gating charges in voltage sensors. *Nature.* 444:775–779.

Simons, K., and G. van Meer. 1988. Lipid sorting in epithelial cells. *Biochemistry.* 27:6197–6202.

Smith, J.J., S. Alphy, A.L. Seibert, and K.M. Blumenthal. 2005. Differential phospholipid binding by site 3 and site 4 toxins. Implications for structural variability between voltage-sensitive sodium channel domains. *J. Biol. Chem.* 280:11127–11133.

Stith, B.J., J. Hall, P. Ayres, L. Waggoner, J.D. Moore, and W.A. Shaw. 2000. Quantification of major classes of *Xenopus* phospholipids by high performance liquid chromatography with evaporative light scattering detection. *J. Lipid Res.* 41:1448–1454.

Suchyna, T.M., S.E. Tape, R.E. Koeppe II, O.S. Andersen, F. Sachs, and P.A. Gottlieb. 2004. Bilayer-dependent inhibition of mechanosensitive channels by neuroactive peptide enantiomers. *Nature.* 430:235–240.

Swartz, K.J. 2007. Tarantula toxins interacting with voltage sensors in potassium channels. *Toxicon.* 49:213–230.

Swartz, K.J., and R. MacKinnon. 1995. An inhibitor of the Kv2.1 potassium channel isolated from the venom of a Chilean tarantula. *Neuron.* 15:941–949.

Swartz, K.J., and R. MacKinnon. 1997a. Hanatoxin modifies the gating of a voltage-dependent K^+ channel through multiple binding sites. *Neuron.* 18:665–673.

Swartz, K.J., and R. MacKinnon. 1997b. Mapping the receptor site for hanatoxin, a gating modifier of voltage-dependent K^+ channels. *Neuron.* 18:675–682.

Takahashi, H., J.I. Kim, H.J. Min, K. Sato, K.J. Swartz, and I. Shimada. 2000. Solution structure of hanatoxin1, a gating modifier of voltage-dependent K^+ channels: common surface features of gating modifier toxins. *J. Mol. Biol.* 297:771–780.

Tombola, F., M.M. Pathak, and E.Y. Isacoff. 2005. How far will you go to sense voltage? *Neuron.* 48:719–725.

Wang, J.M., S.H. Roh, S. Kim, C.W. Lee, J.I. Kim, and K.J. Swartz. 2004. Molecular surface of tarantula toxins interacting with voltage sensors in K(v) channels. *J. Gen. Physiol.* 123:455–467.

Wee, C.L., D. Bemporad, Z.A. Sands, D. Gavaghan, and M.S. Sansom. 2007. SGTx1, a Kv channel gating-modifier toxin, binds to the interfacial region of lipid bilayers. *Biophys. J.* 92: L07–L09.

Winterfield, J.R., and K.J. Swartz. 2000. A hot spot for the interaction of gating modifier toxins with voltage-dependent ion channels. *J. Gen. Physiol.* 116:637–644.